EUROPEAN COMMISSION

Community Research

SEVENTH FRAMEWORK PROGRAMME

ARCHER

Collaborative Project

Co-funded by the European Commission under the
Euratom Research and Training Programme on Nuclear Energy
within the Seventh Framework Programme

Grant Agreement Number: 269892
Start date: 01/02/2011 Duration: 48 Months

www.archer-project.eu

Archer
Advanced Reactor for Cogeneration of Heat & Electricity-R&D

D22.23: TORT-TD/ATTICA3D water ingress models and assumptions for calculation

Janis Lapins, Johannes Bader, Michael Buck (all USTUTT-IKE)

ARCHER project – Contract Number: 269892
Advanced High-Temperature Reactors for Cogeneration of Heat and Electricity R&D
EC Scientific Officer: Dr. Panagiotis Manolatos

Document title	TORT-TD/ATTICA3D water ingress models and assumptions for calculations
Author(s)	Janis Lapins (USTUTT), Johannes Bader (USTUTT), Michael Buck (USTUTT)
Number of pages	30
Document type	Deliverable
Work Package	WP22
Document number	D22.23 – revision 0
Issued by	USTUTT-IKE
Date of completion	15/08/2012
Dissemination level	Restricted to the partners of the ARCHER project

Summary

This document contains an overview of the models used for simulation of water ingress into HTRs. The reaction rates that were found in experiments are presented and described briefly. Also the new treatment of additional gas species that comprise new material properties such as viscosity, heat capacity, heat conductivity and effective diffusion coefficients is summarised.

Approval

Rev.	Short description	First author	WP Leader	SP leader	Coordinator
0	First issue	Lapins (USTUTT-IKE) 15/08/2012		N. Kohtz (TUV) 31/12/12	S. de Groot (NRG 31/12/12

Distribution list

Name	Organisation	Comments
P. Manolatos	EC DG RTD	
All technical participants	ARCHER	
Steering Committee members	ARCHER	

Table of contents

1 Introduction

The aim of this task is to establish a state-of-the-art analysis chain for the safety relevant analysis of water ingress events into an High Temperature Gas-cooled Reactor (HTGR). The computational analysis of water ingress to the reactor core of an HTGR has not been improved in the last decades because the prevailing HTGR designs did not use steam generators for power conversion. Recent developments, however, aim again at producing steam for generation of electricity or supply of process heat.

IKE is further developing the three-dimensional thermal hydraulic code ATTICA-3D (Advanced Thermal hydraulic Tool for In-vessel and Core Analyses). ATTICA-3D is designed to model heat and mass transport in HTRs with pebble or block fuel elements. It allows the calculation of concentrations for an arbitrary number of gas components, taking into account convection and diffusion as well as sources/sinks from chemical reactions.

A basic model of carbon chemistry (reactions with oxygen and steam) is currently being implemented. The coupling with the transient neutron transport codes DORT-TD and TORT-TD (developed by GRS) is currently being implemented in the frame of a nationally sponsored project.

Within this task the ATTICA-3D/TORT-TD code combination shall be used for calculation of water ingress scenarios with particular emphasis on:

- Reactivity effects (heterogeneous temperature model of the fuel element is implemented for spheres, work for block type fuel elements is ongoing)
- carbon chemistry
- estimation of the source term for combustion in the containment/reactor building (formation of combustible gases in the vessel)

2 Calculation Methods

2.1 Pre-processing Codes ZIRKUS and MCNP

The code system ZIRKUS/THERMIX [1] is used to calculate the cross sections of the reference case. ZIRKUS is a 2D modular code system, including a pebble flow module, neutron diffusion module and burnup module. Thermal Hydraulic feedback is given by THERMIX/DIREKT. Group cross sections are achieved by the coupled spectral code MICROX2 from the PSI [2]. The ZIRKUS cross sections are also used for the coupled ATTICA3D/TORT-TD calculations.

MICROX2 explicitly considers the double heterogeneous nature of the fuel (fuel particles in a graphite shell, see Figure 6) and its effect on spectral calculations. The simulation chain of cross sections generation, flux and burnup calculation is necessary to achieve the in situ cross sections.

The Monte-Carlo N-Particle Code (MCNP) is a well-known general code for transport problems [3].

The Code allows detailed analysis of various geometries. The geometry of the fuel pebbles, including the fuel particles, can be explicitly modelled in MCNP, as well as different possibilities for their arrangement in the pebble bed. Point wise cross sections and different material compositions of the fuel particles allow the evaluation of different burnup states.

2.2 Transport and Diffusion Code TORT-TD

For other neutronic calculations of this task, especially 3D evaluations, the time-dependent 3-D fine-mesh few-group discrete ordinates (S_N) neutron transport code TORT-TD is used.

The neutron transport code TORT-TD is being developed at GRS [5]. It is based on the DOORS steady-state neutron transport code TORT [4] and solves the steady-state and time-dependent few-group transport equation with an arbitrary number of prompt and delayed neutron precursor groups in both Cartesian and cylindrical (r-φ-z) geometry. Unconditional numerical stability in transient calculations is achieved using a fully implicit time discretization scheme. Scattering anisotropy is treated in terms of a Legendre scattering cross section expansion. Computing time can be saved by extrapolating the angular fluxes to the next time step using the space-energy resolved inverse reactor period. The features of TORT-TD further include:

- 64 bit encoding to meet imposed tight convergence criteria and to enable TORT-TD to be applied to large realistic problems exceeding 32 bit RAM limitations;
- Movements of single control rods or control rod banks;
- Processing of parameterized tabulated cross section libraries for up to 5 state parameters; interpolation either linear or with cubic spline polynomials, thus allowing to study the impact of different interpolation schemes on cross section evaluation;
- Time-dependent anisotropic distributed external source;
- Leakage and buckling calculation over larger spatial regions (e.g. spectral zones) using the neutron current density in discrete ordinates representation;
- Calculation of Xenon/Iodine equilibrium and transient distribution as a prerequisite for operational transients;
- Fully integrated 3-D fine-mesh few-group diffusion solver (steady state and time-dependent) in both Cartesian and cylindrical geometry.

TORT-TD has recently been extended by a 3-D fine-mesh few-group solver for the steady state and time dependent diffusion equation in few energy groups for both Cartesian and cylindrical (r-ϑ-z) geometry. The diffusion solver is fully integrated in TORT-TD and can be invoked by a single parameter in the input data set. Since it operates on the same spatial discretization and the same cross section data, the diffusion solver allows studying the impact of the diffusion approximation by directly comparing with the S_N solution. It can also be applied to fast running scoping calculations, especially for transients, or as a preconditioner to accelerate subsequent discrete-ordinates calculations.

2.3 Thermal Hydraulics Code ATTICA3D

The ATTICA3D Advanced Thermal Hydraulics Tool for In-vessel and Core Analysis in 3 Dimensions, developed at IKE of Stuttgart University applies the porous medium approach in both cylindrical and Cartesian geometry [6]. Subdivision between solid and fluid fraction in a considered control volume is done via the porosity parameter ε assuming thermal non-equilibrium. Multiple gase phases are foreseen in ATTICA3D.

For the solid structures, the transient energy equation is

$$(1-\varepsilon)\frac{\partial}{\partial t}(\rho_s h_s) = (1-\varepsilon)\nabla\left[\cdot\, \lambda_{s,eff} \cdot \nabla T_s\right] - \dot{q}_{conv} + \dot{q}_{nu}$$

where the index s indicates the solid state, ε, ρ, h, λ_{eff}, Ts, $\dot{q}_{conv}$ and $\dot{q}_{nu}$ denote porosity, density, enthalpy, effective heat conductivity, temperature, convective heat transferred between solids and gases, and the amount of generated nuclear power, respectively.

The time-dependent energy equation for the gas phases is

$$\varepsilon \frac{\partial \rho_g h_g}{\partial t} + \varepsilon \, div\,(\rho_g \vec{u} h_g) = \varepsilon \, div\,(\lambda_{g,eff} \, grad\,(T_{g,i})) + \dot{q}_{conv}$$

where the index $_{g,i}$ indicates gas phase of the gas type $_i$ (e.g. Helium, Oxygen), h is the specific gas enthalpy, $\vec{u}$ denotes the velocity vector, $\lambda_{g,i,eff}$ the effective heat conductivity of the gas and Tg,i the gas temperature. The latter is calculated by

$$\dot{q}_{conv} = \alpha(T_s - T_g)$$

where α is the heat transfer coefficient. Heat transfer within the pebble bed is determined according to KTA standards [7] using the Zehner-Schlünder and, for elevated temperature levels, the Robold correlation.

The mass conservation is only solved for the fluid region. The implemented mass conservation equation comes as

$$\varepsilon \frac{\partial \rho_i}{\partial t} + \varepsilon \, div\,(\rho_i \vec{u}_i) = 0$$

with the same declarations as stated above.

The momentum equation has the form of a simplified equation of Ergun type for porous medium. Since the porous medium approach is strongly dominated by pressure loss, fluid-solid friction and body force, the unsteady and convection term on the left hand side, and on the right hand side diffusion of momentum, additional viscous term are neglected, yielding

$$\varepsilon \, grad\; p = -\vec{R} - \varepsilon \rho_i \, \vec{g}$$

with $\vec{R}$ denoting the friction force, and $\vec{g}$ denoting gravitational acceleration.

To capture the feedback of thermal hydraulics on neutronics a quasi-steady-state heterogeneous temperature model (HTM) for the fuel pebble (see Figure 1) is implemented. This consideration is necessary, since fission heat is mainly generated in the uranium kernel and not in the surrounding graphite. In fast transients, the temperature difference between the fuel kernel and graphite can be substantial. This pronounces strong feedback effects from the fuel Doppler temperature.

In the HTM, the fuel is subdivided into an arbitrary number n of spherical shells, see Figure 1, in our example n = 6.

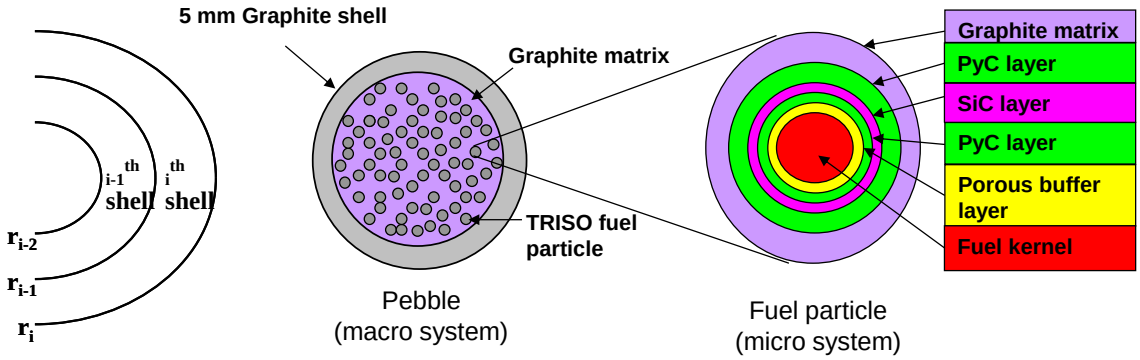

Figure 1 : Subdivision of a fuel element when applying the heterogeneous temperature model

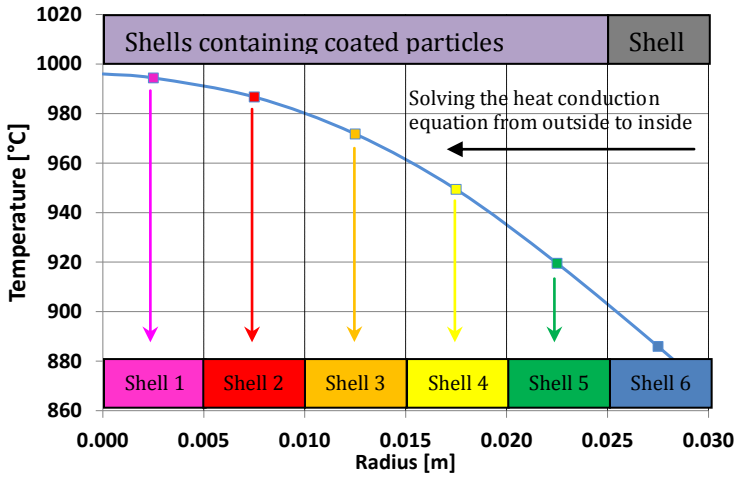

Figure 2 : Temperature distribution after solving the heat conduction equation for the fuel pebble (macro system), delivering boundary conditions for the micro system

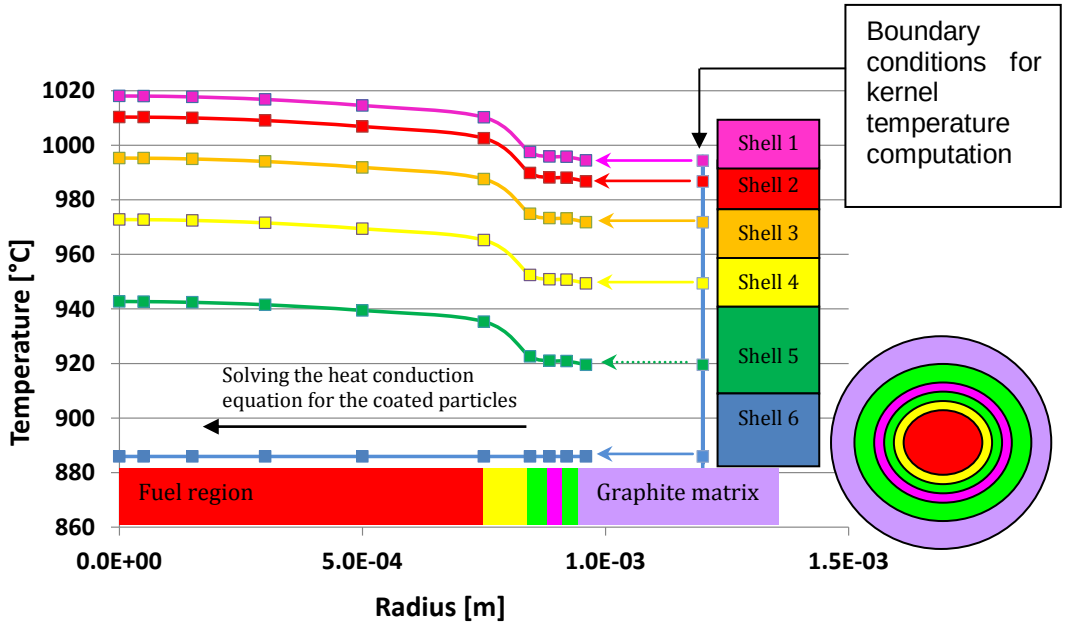

Figure 3 : Temperature distribution for the representative kernels per shell (micro system). The blue bar on the right side visualises the boundary condition after solving

the heat conduction equation and is coloured as in the macro system. The colouring at the bottom display the different coatings according to Figure 2

Starting from the surface of the fuel element (kth shell or graphite matrix, here k = 6), the steady-state heat conduction equation for each shell is solved towards the fuel element centre (k-1st shell, then k-2nd shell and so on). The surface temperature of the fuel element is taken as the boundary condition. Mean temperatures are calculated for successive fuel shells, until the innermost shell. These temperatures, however, only apply to the graphite shells (macro system), not the fuel kernels (micro system).

For the average temperature of the fuel particles contained in a considered shell, a representative particle is determined that gets appointed the mean temperature for all the fuel kernels contained within. In order to determine the representative particle temperature, the respective shell temperature of the surrounding graphite serves as boundary condition.

Here, the heat conduction equation is solved for the micro system once more, taking into account the different heat conductivities of the coatings of the particles. After fuel and moderator temperatures are determined, the temperature values are averaged and one fuel temperature and moderator temperature per thermal hydraulic mesh is obtained to process nuclear cross sections. Thus, fuel temperature feedback is much more pronounced than it is without HTM. In Figure 2 and Figure 3, typical temperature profiles during steady-state are presented for a pebble in the central bottom part of the reference plant.

In order to correctly account for variation of material properties, ATTICA3D comes with a large material properties library. For the description of other phenomena like heat transfer outside the pebble bed, pressure losses due to changing diameters in the flow path, thermal radiation and so on, a set of constitutive equations are provided within ATTICA3D.

Technically, the coupled code system TORT-TD/ATTICA3D is represented by a single executable in which ATTICA3D acts as the main program and calls TORT-TD in terms of a subroutine whenever an update calculation of the power distribution is requested. For the data exchange between TORT-TD and ATTICA3D, already existing TORT-TD interface routines have been utilized in combination with the ATTICA3D mesh overlay feature that transfers 3-D distributions from its thermal-hydraulic mesh to a superimposed neutron-kinetics mesh and vice versa. This allows for efficient data transfer via direct memory access of array elements.

A TORT-TD/ATTICA3D transient simulation consists of a three-step procedure. First, a coupled steady state calculation is performed. ATTICA3D and TORT-TD are called repeatedly, followed by exchange of thermal-hydraulic and neutron kinetics data, until convergence of the 3-D temperature and power distributions are achieved. At the beginning of the iteration process, TORT-TD calculates for a given thermal-hydraulic initial distribution the corresponding power distribution that is transferred to ATTICA3D as first estimate. Second, a zero transient follows based on the converged steady state with no changes being imposed on the system. A few seconds zero transient may help verify the stability of TORT-TD and ATTICA3D when both codes switch to their respective time-dependent mode of operation. In the last step, the actual transient is being initiated.

3 Description of Reference Plant

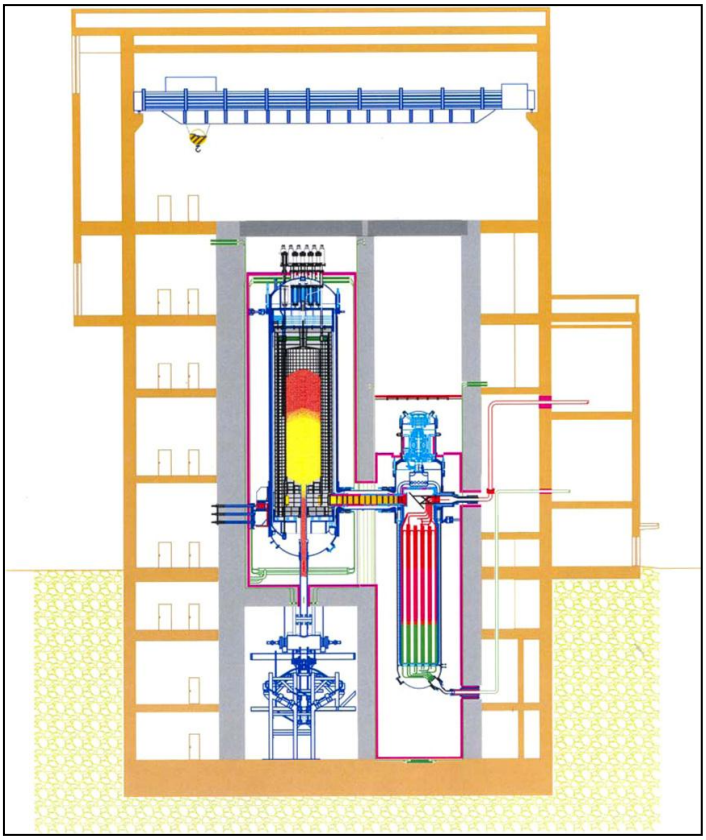

Figure 4 : Cross section of HTR-PM building with primary cavity (reactor pressure vessel, steam generator)

The only HTR concept at the brink of finalization at the moment is the Chinese HTR-PM (Figure 4), which stands for High Temperature Reactor – Pebble Bed Modular. It was developed after the successful test with the HTR-10 test reactor and is based on HTR-Modul designed in Germany by Siemens-Interatom in the 1980s [8]. It was decided that a pebble bed reactor based on the HTR-PM the ***ARCHER Reference Plant*** (ARP) will be selected as a reference case for further calculations.

The layout of the ARP is therefore a one zone cylindrical core consisting of a pebble bed (Figure 4, Figure 5). To compete economically with current Light Water Reactor (LWR) designs, two or more reactor cores should be coupled to one power conversion unit (turbine). To benefit from existing equipment, the power conversion is a Rankine Process (steam turbine) which includes a steam generator at the reactor.

A central graphite structure consisting of a fixed structure or moderator pebbles is not foreseen. The core has a diameter of 3 m which is the same as the HTR-Modul (Table 1). The height of the flattened core is 11m. With an estimated average porosity of 0.39 of the pebble bed there are approximately 420,000 pebbles in the reactor. The Helium pressure in the primary loop is 7 MPa. The Helium in the primary loop flows from the steam generator with a temperature of 250°C and a rate of 96.3 kg/s through a coaxial pipe, through the helium risers to the top of the core, from there through the pebble bed downwards and the porous bottom reflector with a temperature of 750°C back to the steam generator. The control rods (CRs) consist of multiple B4C rings hanging from the top of the reactor (Figure 7). Each CR can be driven independently. In case of a station blackout, the control rods fall into their shut-down position by gravity. As secondary and additional shut-down system, small absorber spheres (SAS) with a diameter of 1cm can fall by gravity (withheld by electrical valves) into long holes in the side reflector (Figure 8). The side reflector has a thickness of 75cm (this includes borated carbon bricks with a thickness of 5cm to protect the outer

components of the reactor). The side reflector is dived into 30 azimuthal sections, each with either a CR-hole or two long holes for the SAS (hole circle diameter for both 162.5cm).

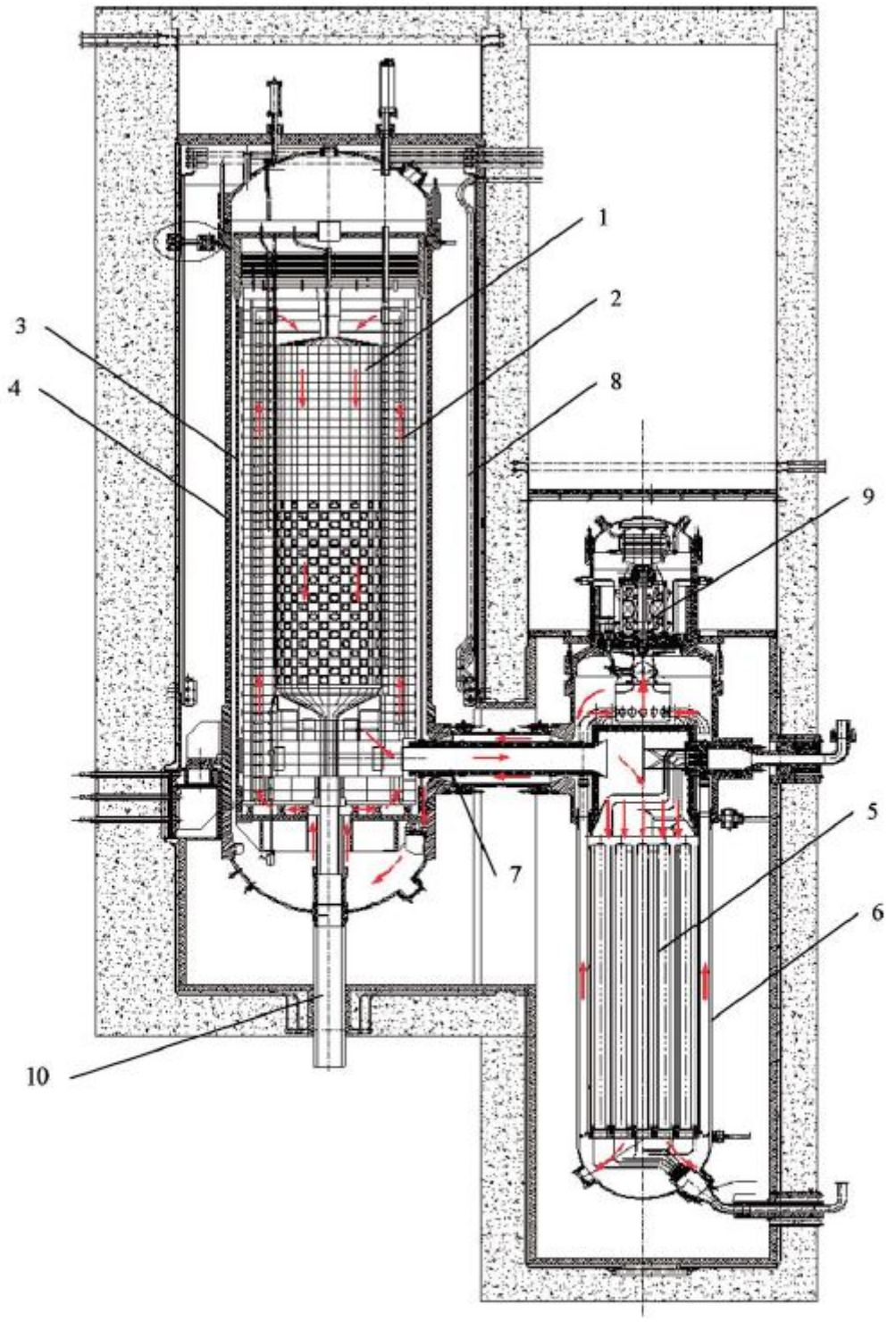

Fig. 1 Cross-section of the HTR-PM reactor: (1) reactor core, (2) side reflector and carbon thermal shield, (3) core barrel, (4) reactor pressure vessel, (5) steam generator, (6) steam generator vessel, (7) coaxial gas duct, (8) water-cooling panel, (9) blower, (10) fuel discharging tube, (11) control rod driving system, and (12) small absorber sphere unit

Figure 5 : Cross section of HTR-PM

The graphite components are kept in shape by a core barrel made of steel, which is then surrounded by a carbon structure. The whole setup is situated inside a Reactor Pressure Vessel (RPV) made of steel. At the outside of the RPV the Reactor Cavity Cooling System (RCCS) is installed, which protects the reactor structures from temperature induced damage during accidents by transporting the expected excessive heating power.

The fuel of the reactor consists of fuel pebbles made from graphite, which include fuel particles with a diameter of 500µm (Figure 6). The particles have different coatings, namely a buffer graphite coating to absorb gaseous fission products, a binder coating to the Silicon-Carbide coating and another binding layer (TRISO). The Silicon carbide coating is intended to sustain the fission products during an accident with a assumed heating up of the core. The main fuel parameters can be found in Table 2.

Table 1 : Main design parameters

Parameter	Unit	Value
Rated electrical power	MW	110
ReactorThermal Power	MW	250
Average core power density	MW/m^3	3.22
Eletrical Efficency	%	42
Primary helium pressure	MPa	7
Helium temperature at reactor inlet/outlet	°C	250/750
Helium flow rate	kg/s	96.3
Numer of Helium riser channels	-	30
Active core diameter	m	3
Equivalent core height	m	11
Height upper void	m	0.57
Number of control rods	-	8
Diameter of control rod holes	cm	65
Number of SAS	-	2x22
Type of steam generator	-	Once through helical coil
Main steam pressure	MPa	13.24
Main steam temperature	°C	566
Main feed-water temperature	°C	205
Main steam flow rate at the inlet of turbine	t/h	673

Table 2 : Main fuel element parameters

Parameter	Unit	Value
Fuel Type	-	TRISO
Heavy Metal (HM)	-	UO2
Radius of U- Kernel	µm	250
Thickness of the 4 Kernel Layers	µm	95 / 40 / 35 / 35
Density of HM-Oxide	g/cm3	10.4
Density of the 4 Coatings	g/cm3	1.05 / 1.9 / 3.18 / 1.9
Radius of Fuel Matrix	cm	2.5
Radius of Fuel Element	cm	3.0
Graphite Density of Matrix	g/cm3	1.74
HM per fuel element	g	7
Enrichment of fresh fuel	%	8.9
Thermal absorption cross section of Graphite [Fuel and Reflector]	mbarn	4
Number of fuel elements in reactor core	-	420,000

Average burn-up	GWd/tU	90
Pebble-bed porosity	-	0.39
Fueling mode	Multipass	15

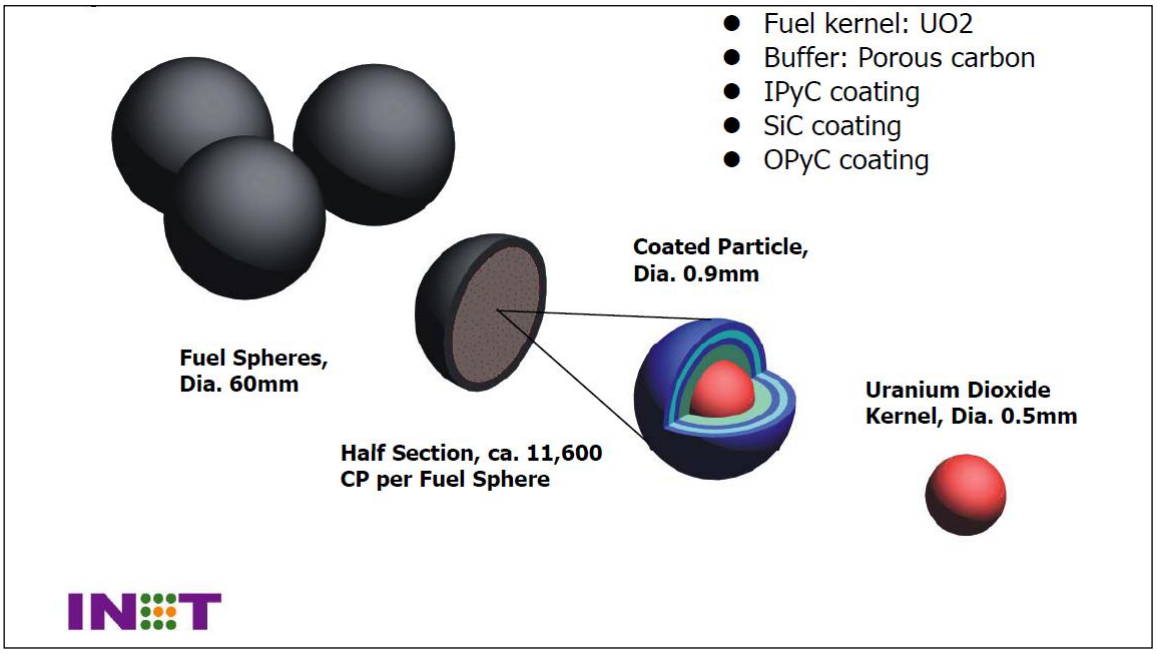

Figure 6 : Layout of fuel Elements

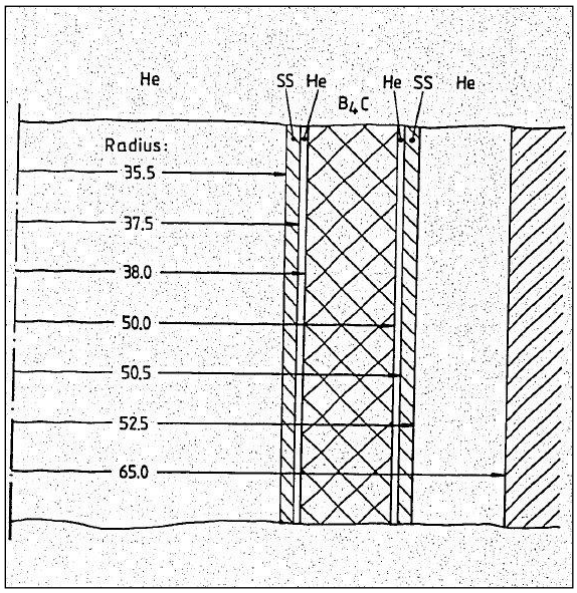

Figure 7 : Control Rod layout (SS : Stainless Steel)

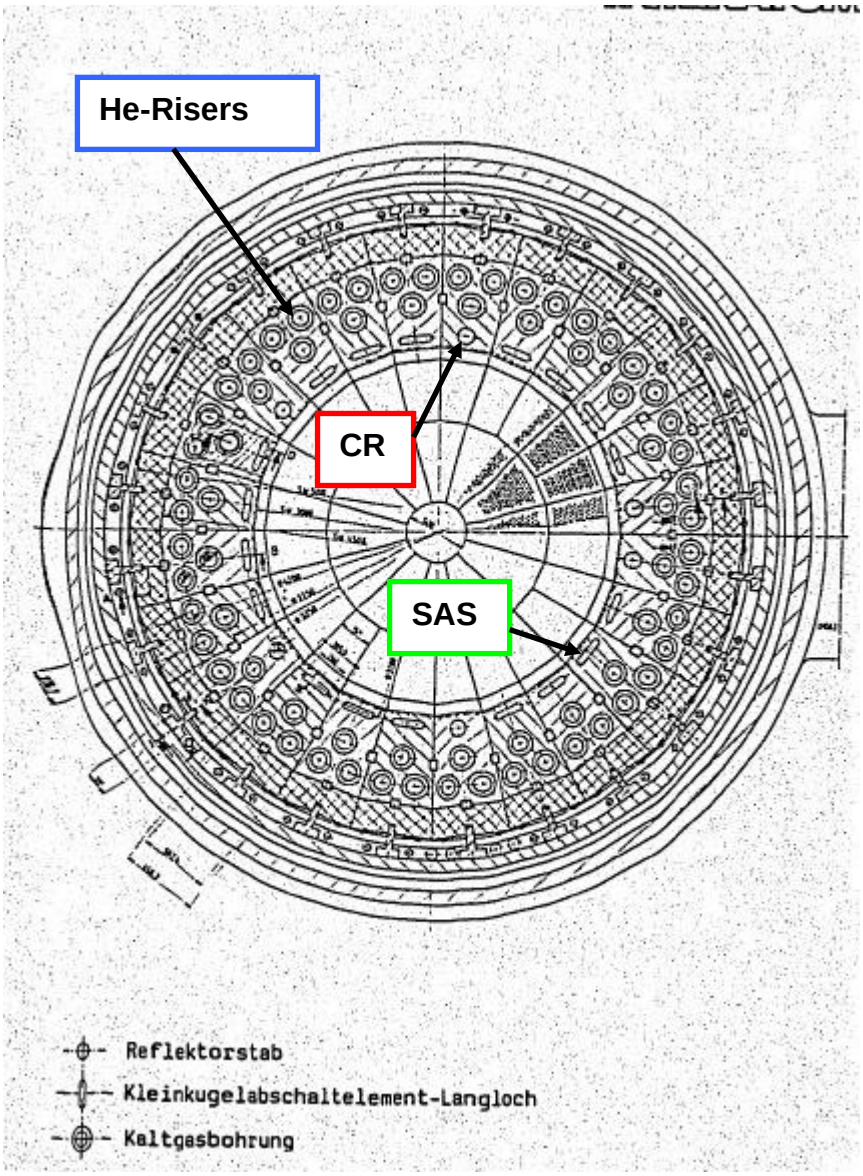

Figure 8 : Horizontal cross section of HTR-Modul with Helium risers, control rod holes and small absorber sphere holes

4 Water Ingress

Water ingress can cause serious safety concerns for HTRs and may occur as a consequence of a tube rupture inside the steam generator. This is an event that can occur during life-time and is an accident that should be accounted for on design basis, since tube ruptures in light water reactors do occur from time to time and cannot be excluded. In an HTR with steam generator, the pressure of the secondary circuit is higher than in the primary circuit. In the reference plant case, the primary pressure is 70 bars whereas the secondary pressure amounts to 139 bars. From the safety point of view, there are two major effects to be considered: Reactivity effects and the corrosion of graphite structures in combination with possible formation of explosive gas mixtures.

- Reactivity effects: HTRs are usually under-moderated to achieve reasonable burn-up and accommodate the fuel reload system. With steam or water ingression into the core, a lot of moderator is added making the moderation ratio more favourable for neutronics. This leads to an increased number of fissions yielding a power increase of the whole reactor. In case of water intruding the core the positive feedback from the moderator has to be compensated with a negative fuel temperature effect, otherwise the coatings of the particles will fail and radioactive fission products will be released into the primary circuit. A wash-out of fission products which tend to be bound to graphitic dust may occur due to presence of steam or water. In order to simulate the consequences of ingress of additional moderator, the parameters to take into account in the cross section processing will be increased by introducing a further parameter that has to be varied.

- Corrosion effects: The adding of hot water or steam, respectively, is supposed to lead to moderate corrosion at the graphite structures or in the pebble bed.

4.1 Neutronic Treatment of Water ingress

In order to account for increasing moderation due to steam or hydrogen within the core region, appropriate nuclear cross-sections have to be processed. Therefore, the NEA code MICROX2 which is integrated in the ZIRKUS neutronics code system is used to generate these cross sections that are subsequently used for transient calculations in TORT-TD. 13 energy groups are considered. This makes the buckling dependency unnecessary. Only with a small number of energy groups, the bucklings have to be included. The cross sections can be parameterised with respect to fuel and moderator temperature, fast and thermal buckling, xenon density and now, additionally, also hydrogen content, but bucklings will be left out. For the generation of cross sections within the core region the variation is described in Table 3

Table 3 : Dependencies of nuclear cross sections for TORT-TD (water ingress):

Variation parameter	Unit	Number of supporting points	Supporting points
Fuel temperature	K	10	300, 500, 700, 900, 1100, 1300, 1500, 1700, 1900, 2100
Moderator temperature	K	7	300, 600, 900, 1200, 1500, 1800, 2100
Buckling	-	0	-
Xenon density	$(barn^* cm)^{-1}$	3	0.0, 2.0E-11, 8.0E-10
Water content	kg	4	0, 200, 500, 800

Depending on the thermal hydraulic and neutronical state, each group cross section has 10 * 7 * 3 * 4 = 840 variations. In between the above mentioned values, the cross sections are interpolated. There is also a slight overhead of data because some states are not likely to occur at any time, i.e. moderator temperature (2100 K) much higher than fuel temperature (300 K).

As a rough basic assumption, the maximum amount of water in the core region is determined by:

$$p \cdot V = m \cdot R \cdot T$$

Gas volume in core

$$V_{Core\_gas} = \pi \cdot r^2 \cdot h \cdot 0.39 \approx 30.3 m^3$$

Mean temperature (arithmetical mean of inlet and outlet gas temperature)

$$T = \frac{T_{out} + T_{in}}{2} = 773 \ \ K$$

The specific gas constant for steam is R_{H2O} = 462 J/ (kg* K) and the secondary train of the safety and relief valve opens at 82.5 bars (12.5 bar overpressure), see [13]. This yields an approximate steam content of:

$$m = \frac{p \cdot V}{R_s \cdot T} = \frac{82.5 \cdot 10^5 \frac{kg}{m \cdot s^2} \cdot 30.3\, m}{462 \frac{J}{kg \cdot K} \cdot 773 K} \approx 700\ kg$$

But one has to keep in mind that this is only the case if all helium would be driven out of the system and the steam takes over all the available gas space (steam filling of 100%). The value of 800 kg – an extra 100 kg is used for conservatism - is therefore used as the maximum possible steam mass within the core for the cross section processing.

The assumption of steam being an ideal gas surely bares errors. The water entering the primary circuit from the steam generator is not completely evaporated at once; part of it enters as steam more comes in liquid state [13]. Flash evaporation can occur. Assuming constant evaporation rates (e.g. 5 kg/s) in the beginning, a certain concentration will the core. Only when this first steam front returns to the steam generator again (after seconds), it will be increased by the previous amount. It is very likely that the first steam front will already increase the reactor power considerably. This will, in turn, lead to a rise of temperature. The inlet and outlet temperature assumption will not hold anymore. Overall temperatures will increase. Due to the rotation of the blower droplets are effectively separated from the steam. Due to the elevated temperatures within the graphite structure the water will not remain in a liquid state.

When TORT-TD executes a computational step, parameters depending on the thermal fluid mechanics are transferred from ATTICA3D to TORT-TD via a common interface (fuel and moderator temperature, hydrogen density). When TORT-TD receives the respective values, the appropriate cross-section is interpolated for the core and reflector zones. The bucklings as well as the xenon density are determined by TORT-TD itself.

One could also think to include both steam and hydrogen densities at the cost of higher computational times.

4.2 Corrosion of graphite with steam

4.2.1 Theoretical background

Compared to air ingress, the corrosion in steam atmosphere is rather moderate. The probability of reaction at 800°C, normalised on the graphite-oxygen reaction are presented in the table below, see [14]

Table 4 : Likelihood of reactions at 800°C

Reaction between	Relative reaction rates
O2 + Graphite	1
Steam + Graphite	3.0×10^{-5}
CO2 + Graphite	1.0×10^{-5}
Hydrogen + Graphite	3.0×10^{-8}

But usually, the water ingress takes place in a pressurised case whereas air ingress usually follows a depressurisation. The reactions that are considered are presented in Table 5

Table 5 : reactions considered in the water ingress

Reaction	ΔH
H2O + C ←→ H2 + CO	+ 131.3 kJ/mol
H2O + CO ←→ H2 + CO2	- 41.2 kJ/mol
CO2 + C ←→ 2 CO	+ 172.5 kJ/mol

Additionally, methane production can also become important when hydrogen partial pressures is high.

2 H2 + C ←→ CH4, ΔH = - 74.85 kJ/mol

With knowledge of one reacting component, the others can be derived through stoichiometry. That yields as reaction rates n' (mol current) or m' (mass current) for

1. the reaction rate of steam with graphite

   $\dot{n}_{H2O} = \dot{n}_C$

2. the reaction rate of the produced hydrogen

   $\dot{n}_{H2} = -\dot{n}_{H2O}$

3. the reaction rate of produced CO

   $\dot{n}_{CO} = \dot{n}_{H2O}$

4. and for the reaction rate of the hydrogen

$$\dot{n}_{H2} = \dot{n}_{CO2}$$

For the respective mass current the mol currents have to be multiplied by the mol masses.

The reactions that take place can be subdivided in three ranges, see Figure 9, Figure 10:

- Chemical regime, Graphite temperatures < 850 °C: the gases diffuse fast enough to give a uniform homogeneous corrosion within the graphite
- In-pore diffusion regime, graphite temperatures between 850 and 1200 °C : the reaction speed is high enough that oxygen cannot diffuse throughout the whole graphite, a corrosion profile is the consequence
- Boundary layer diffusion controlled regime: graphite temperatures > 1200°C, here, the temperature is so high, that virtually all oxidation takes place in a small boundary layer outside the surface of the graphite

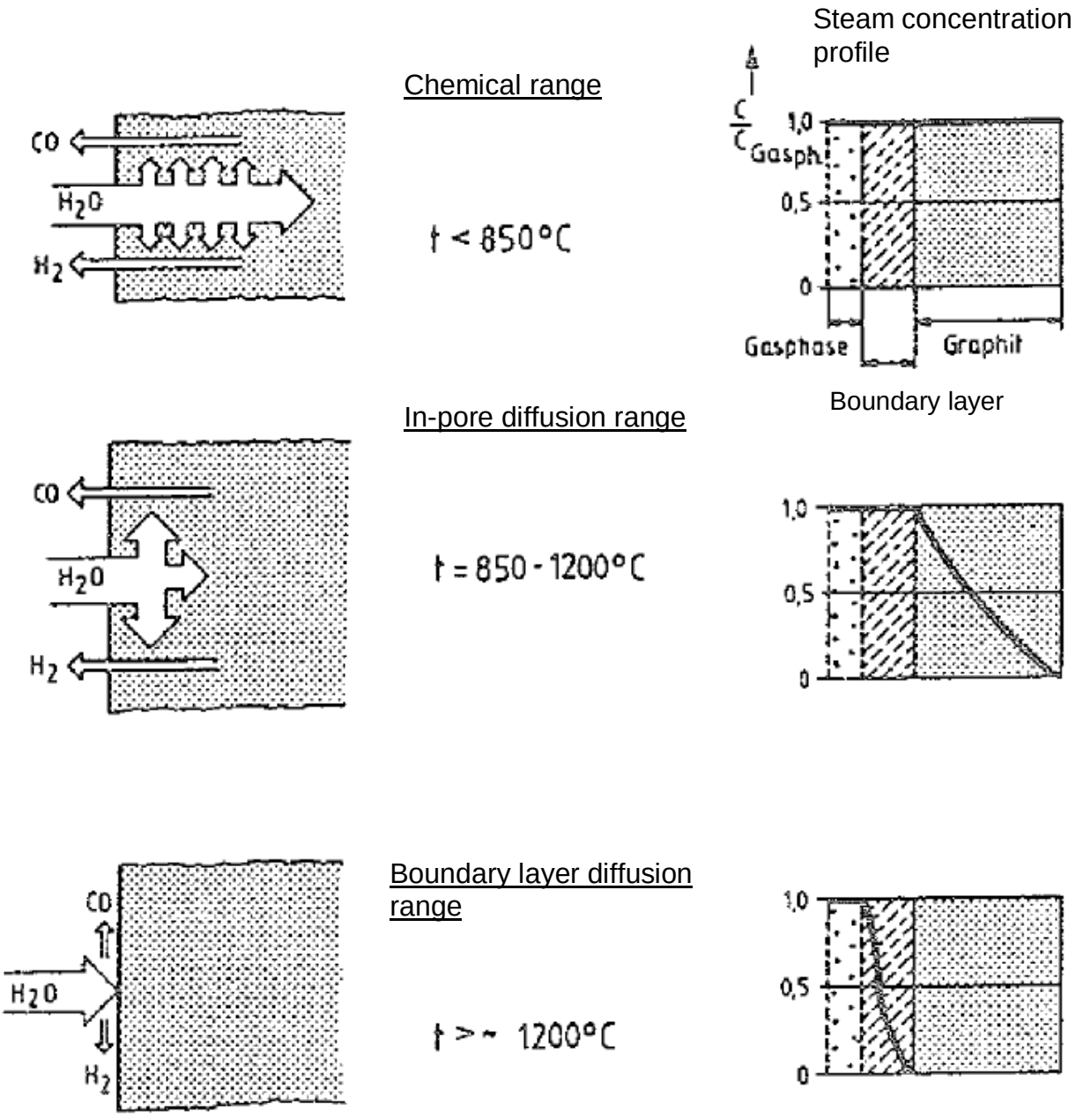

Figure 9: Different ranges for the chemical reaction of graphite with steam [15]

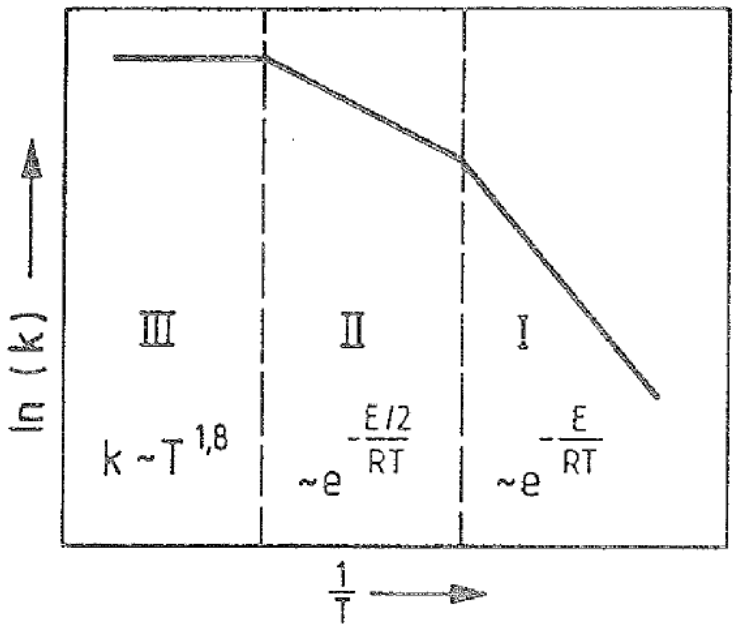

Figure 10 : Logarithmic reaction rates over reciprocal temperature [15]

The temperature is the most important parameter for the corrosion processes. But there is a multitude of other dependencies. These are subsequently presented in an order that represents the importance of the respective parameter:

1) Temperature
2) System pressure
3) Steam concentration
4) Burn-off of graphite (opening of internal pores)
5) Activation energy
6) Catalysts
7) Inhibitors
8) Neutron irradiation
9) Flow velocity

Some of these parameters of influence are very hard to determine, need a lot of experiments and are certainly not to extrapolate for different kinds of graphite. That makes a detailed description hard to realise. In order not to under-estimate any graphite corrosion effects it is safer to apply higher values (e.g. for the burn-off of graphite) from the beginning. This may lead to an over-prediction of the corrosion or an earlier failure of the material under consideration.

Chemical reactions generally obey Arrhenius' law,

$$RR = k_0 \cdot \exp\left(-\frac{E_A}{RT}\right)$$

where *RR* denotes the reaction rate, k_0 denotes a frequency factor, E_a is the activation energy, *R* is the general gas constant, and *T* is the temperature.

4.2.2 Determination of material properties of gases and mixtures

In order to determine material properties for the mixture the following correlations are applied.

Heat capacities:

The heat capacities of the mixture (neglecting the mixing enthalpies) are

$$\left(\frac{\partial H}{\partial T}\right)_p = c_p = \sum_j c_{p,k} \cdot x_k \qquad \text{[J/(K·mol)]}$$

where c_p, x_k denote the heat capacity and the mass fraction of the respective gas component *k*.

Viscosities:

For calculation of the viscosity of the single gas components, the Chapman-Enskog theory approach is chosen. This proposes the relation of

$$\eta_k = 8.430 \cdot 10^{-25} \frac{(M_k \cdot T)^{0.5}}{{\sigma_k}^2 \cdot \Omega^{(2,2)}} \qquad \text{[kg/(m·s)]}$$

where M_k is the molar mass, T is the temperature, σ is the collision diameter and with the help of the characteristic interaction energy ε_w the collision integral $\Omega^{(2,2)}$ can be calculated. $\Omega^{(2,2)}$ is a function of temperature and the interaction energy ε_w.

For the helium properties, the recommendations of the KTA (German Nuclear Safety Standard Commission) are used.

The viscosity of the gas mixture is computed according to Brokaw [17] which has a good agreement with experimental data.

Heat conductivities

For monoatomic gases, there is a dependence of the heat conductivity on the viscosity, namely

$$\lambda_k = 3.75 \cdot \frac{R}{M} \cdot \eta_k \qquad \text{[W/(m·K)]}$$

where R is the gas constant, M is the molar mass, and η is the viscousity of the respective material.

For gases that consist of more than just one atom, a correction has to be applied that accounts for the energy transfer from the rotational and vibrational degrees of freedom to the translational. This correction increases the conductivity and was introduced by Eucken

$$\lambda_{EU,k} = 0.88 \cdot \left(0.4 \frac{c_{p,k}}{R} - 1\right) \cdot \lambda_k \qquad \text{[W/(m·K)]}$$

where c_p is the heat capacity, R is the gas constant and λ is the heat conductivity of the gas.

The helium heat conductivity is calculated according to KTA standard 3102.3.

The heat conductivity of the gas mixture is computed according to Brokaw [17].

Diffusion coefficients

According to Chapman-Enskog theory the computation of the binary diffusion coefficients is done using, see [16]

$$D_{jk} = 5.954 \cdot 10^{-24} \cdot \frac{\Theta_{jk}^{0.5} \cdot T^{1.5}}{P \cdot \sigma_{jk}^{\ 2} \cdot \Omega^{(1,1)}} \quad \left[\frac{m^2}{s}\right]$$

with

The molar mass ratio

$$\Theta_{jk} = \frac{M_j + M_k}{M_j \cdot M_k} \quad \left[\frac{mol}{kg}\right],$$

the mean collision diameter

$$\sigma_{jk} = 0.5 \cdot (\sigma_j + \sigma_k) \quad [m]$$

the collision integral (tabulated)

$$\Omega^{(1,1)} = f\left(\frac{T}{\varepsilon_{w,jk}}\right) \quad [-]$$

and a mean interaction energy

$$\varepsilon_{w,jk} = \left(\varepsilon_{w,j}\varepsilon_{w,k}\right)^{0.5} \quad \left[\frac{J}{mol}\right]$$

From the binary diffusion coefficients one can calculate the diffusion coefficient of the gas mixture with the help of:

$$D_{kM} = \left(1 - x_k\right) / \sum_{j \neq k}^{n} \frac{x_j}{D_{jk}} \quad \left[\frac{m^2}{s}\right]$$

where x_k denotes the mass fraction of the considered gas component k ,x_j denotes the mass fraction of all the other component in the mixture M.

4.2.3 Introducing new gas components, diffusion terms, chemical heat and enthalpy transport into ATTICA3D

In order to capture the produced gas masses additional terms are introduced in the total mass conservation equation. The new terms are marked in red.

Total mass conservation equation:

$$\frac{\partial(\varepsilon\rho)}{\partial t} + div(\varepsilon\rho\vec{u}) = div\left(D_{k,eff}\ grad\ c_k\right) + \sum_{k=1}^{nc}\left(\sum_{n=1}^{nreac}\dot{m}_k^n\right)$$

with $k = 1,...,n_c$, $c_k = \frac{m_k}{m_{total}}$, and $\sum_{k=1}^{n_c} c_k = 1$

Here, on the right hand side two new terms are introduced, the produced gases along with their diffusive transport. $D_{k,eff}$ denotes the effective diffusion constant, c_k as concentration of the component *k* and $\dot{m}_k^n$ as the generated gas mass per second. The sum operator comprises the mass sources from all possible chemical reactions from *1,…, nreac*. Also, for each new gas component *k*, that is water(steam), hydrogen, carbon monoxide and carbon dioxide, a mass conservation each is introduced to ATTICA3D.

Mass conservation equation for the single component:

$$\frac{\partial(\varepsilon\rho c_k)}{\partial t} + div\left(\varepsilon\rho\vec{u}c_k\right) = div\left(D_{k,eff}\ grad\ c_k\right) + \sum_{n=1}^{nreac}\dot{m}_k^n$$

Here, the newly introduced terms are on the right hand side are similar to the total mass equation but only for a single component. In the water ingress case there are four reactions considered (see Table 5). The formation of methane will not be considered in a first approach.

In the energy equations of both solid and fluid new chemical heat sources are introduced. Depending of the nature of the reaction (heterogeneous or homogeneous) different heat sources are used.

In the heterogeneous case, chemical heat will be added to the solid, whereas in the other case the heat is added to the fluid. Unlike in literature, chemical heat by endothermal reactions, will be substracted from the solid or fluid; chemical heat of exothermal reactions are added. For the fluid, an additional enthalpy transport for the different components is considered.

Energy conservation for the gas:

$$\frac{\partial\varepsilon\rho\, h}{\partial t} + div\left(\varepsilon\rho\,\vec{u}h\right) = div(\varepsilon\lambda_{g,eff}\,grad(T_g)) + \dot{q}_{conv} + \sum_{n=1}^{nreac}\dot{q}_{chem,\mathrm{hom}}^{\,n} + \sum_{k=1}^{nc}\sum_{n=1}^{nreac}\dot{m}_k^n h_k$$

Energy conservation for the solid:

$$(1-\varepsilon)\rho_s c_{p,s}\frac{\partial T_s}{\partial t} = (1-\varepsilon)div(\lambda_{eff}\,grad(T_s)) - \dot{q}_{conv} + \dot{q}_{nu} + \sum_{n=1}^{nreac}\dot{q}_{chem,het}^{\,n}$$

The momentum equation is not changed.

In order to obtain the heat produced or consumed by chemical reaction, experimental data had to be obtained. Here, mainly contributions of the Jülich research centre from the early eighties and nineties were used, see [14][15][18][19].

It has to be mentioned that compared to the experiments performed for air ingress only a small data base is available. This is owed to the fact that corrosion with steam has far less tendency to weaken the graphitic parts compared to air ingress.

It could be shown experimentally that the corrosion behaviour can be described best with a Langmuir-Hinshelwood equation. This equation uses Arrhenius terms, but also accounts for inhibiting effects of product and educt gases on certain reactions.

Langmuir-Hinshelwood equation [18]:

$$RR = \frac{k_{01}\exp\left(\frac{-E_{a1}}{R\cdot T}\right)\cdot p_{educt}\cdot f(Burn-off)\cdot p_{total}}{1 + k_{02}\exp\left(\frac{-E_{a2}}{R\cdot T}\right)\cdot\sqrt{p_{educt}} + k_{03}\exp\left(\frac{-E_{a3}}{R\cdot T}\right)\cdot\sqrt{p_{product}}}$$

Here, *RR* is the reaction rate of a component, e.g. graphite reacts with H2O in form of steam, but this reaction will be slowed down by the abundance of hydrogen. k_{01} denotes a so called frequency factors, the exponential term contains the activation energy E_{a1}, the general gas constant and the temperature (Arrhenius term). The Arrhenius term is multiplied by a function of burn-off *f(burn-off)* of graphite. This value ranges from 0.2 for the uncorroded graphite up to 1 for maximum graphite burn-off. The physical reason for this is the opening of previously closed pores within the graphite, offering an increased internal surface for reaction. Also, the partial pressure of the educt and the product are relevant, and the equation can contain a dependence on total pressure p_{total}. In the denominator, one finds two Arrhenius terms multiplied by the partial pressure's square root. Depending on the material and the chemical reaction considered, these inhibiting terms have to be taken into account.

For the different graphite types the corrosion behaviour can vary.

For the modelling of corrosion due to water ingress experimentally determined reaction rates are employed. These comprise the heterogeneous reactions, since the homogeneous reactions (reaction of carbon monoxide with steam) do not depend on the nature of graphite, i.e. the carbon monoxide does not remember its provenience. For the H2O partial pressure range of 0.03 bar < p_{H2O} < 5 bar and a graphite burn-off of approximately 2%, the reaction rate of the graphite.

Primary heterogeneous reaction:

The primary heterogeneous reaction (**C +H2O → CO + H2**) yields a graphite reaction rate RR of:

$$RR_{Graphite} = \frac{6.4\cdot 10^{11}\cdot \exp\left(-\frac{256{,}000}{8.315\cdot T}\right)\cdot p_{H2O}^{0.44}}{1+7.5\cdot 10^{-5}\cdot \exp\left(\frac{121{,}000}{8.315\cdot T}\right)\cdot p_{H2}^{0.9}\cdot p_{H2O}^{-0.4}} \quad \left[\frac{mg}{cm^2\cdot h} = \frac{10^{-2}kg}{3.6\cdot 10^3\ m^2\cdot s}\right]$$

This correlation is taken out of [19] and will be used as graphite corrosion rate. Here, p_{H2}, p_{H2O} denote the partial pressures in **bar**. There are other correlations but these were determined for varying total pressures and graphite burn-off whilst keeping the steam partial pressure constant (at 474 mbar), no partial pressure or temperature dependency is derived, see [20]. Nevertheless, this data can be useful to verify graphite burn-off and total pressure dependencies.

With knowledge of the amount of corroded graphite, the gas masses produced (CO,H2) and consumed (H2O) in the primary heterogeneous water-shift reaction (C + H2O → CO + H2) are easy to determine by stoichiometry. As the units of eq. are given in kg/s, one only has to multiply the gas mass with the mol ratio of molar mass(CO)/molar mass(C) or molar mass(H2)/molar mass(C) to obtain the produced masses in kg/s. Also, the nature of the reaction has to be checked. When 1 mol of CO and H2 are produced each, 1 mol each of H2O and C are consumed. So for known graphite corrosion rates the subsequent produced/consumed gas components are:

$$\dot{m}_{Graphite} = -RR_{Graphite}\cdot surface \quad \left[\frac{kg}{s}\right]$$

For the consumed steam: $$\dot{m}_{H2O} = \dot{m}_{Graphite}\cdot\frac{mol\_mass_{H2O}}{mol\_mass_C} \quad \left[\frac{kg}{s}\right]$$

For the produced hydrogen: $$\dot{m}_{H2} = -\dot{m}_{Graphite}\cdot\frac{mol\_mass_{H2}}{mol\_mass_C} \quad \left[\frac{kg}{s}\right]$$

For the produced carbon monoxide: $\dot{m}_{CO} = -\dot{m}_{Graphite} \cdot \frac{mol\_mass_{CO}}{mol\_mass_{C}} \quad \left[\frac{kg}{s}\right]$

For the chemical heat (endothermal): $\dot{q}_{chem,CO} = \dot{n}_{CO} \cdot \Delta H = \dot{n}_{CO2} \cdot \left(-131.3 \frac{kJ}{mol}\right) \quad [kJ]$

Secondary homogeneous reaction:

The reduction of water in presence of carbon monoxide (**CO + H2O ←→ CO2 + H2**) and vice versa is a well-known reaction and was investigated in [21][22]. This reaction only happens in the interstices of the solid.

For the reaction **CO + H2O → CO2 + H2** the corresponding reaction rates are, see [21][22]:

$$\dot{n}_{CO2} = \frac{2.32 \cdot 10^{14} \cdot \exp\left(-\frac{33{,}000}{T}\right) \cdot c_{H2O} \cdot \sqrt{c_{CO}}}{\sqrt{1 + 1.2 \cdot 10^{4} \cdot c_{H2}}} \quad \left[\frac{mol}{m^3 \cdot s}\right]$$

Note, that the reaction is now given in mol/(m^3 * s).

From the production of CO2 the reaction rates are determined as follows:

$$\dot{m}_{CO2} = \dot{n}_{CO2} \cdot volume \cdot porosity \cdot mol\_mass_{CO2} \quad \left[\frac{kg}{s}\right]$$

with $volume \cdot porosity$ is the gas volume that is left for the secondary reactions. Average porosities e.g. are 0.39 within the pebble bed, 0.2 for the helium risers and so on.

For the H2: $\dot{m}_{H2} = \dot{m}_{CO2} \cdot \frac{mol\_mass_{H2}}{mol\_mass_{CO2}} \quad \left[\frac{kg}{s}\right]$

For the CO: $\dot{m}_{CO} = -\dot{m}_{CO2} \cdot \frac{mol\_mass_{CO}}{mol\_mass_{CO2}} \quad \left[\frac{kg}{s}\right]$

For the H2O: $\dot{m}_{CO} = -\dot{m}_{CO2} \cdot \frac{mol\_mass_{H2O}}{mol\_mass_{CO2}} \quad \left[\frac{kg}{s}\right]$

For the chemical heat (exothermal):

$$\dot{q}_{chem,CO2} = \dot{n}_{CO2} \cdot \Delta H = \dot{n}_{CO2} \cdot \left(41.2 \frac{kJ}{mol}\right) \quad [kJ]$$

For the opposite reaction **CO2 + H2 → CO + H2O**, see [21][22]

$$\dot{n}_{H2O} = \frac{2.9 \cdot 10^{12} \cdot \exp\left(-\frac{28{,}200}{T}\right) \cdot c_{CO2} \cdot \sqrt{c_{H2}}}{1 + 3.6 \cdot 10^{3} \cdot c_{CO}} \quad \left[\frac{mol}{m^3 \cdot s}\right]$$

Here the corresponding equations are

$$\dot{m}_{H2O} = -\dot{n}_{H2O} \cdot volume \cdot porosity \cdot mol\_mass_{H2O} \quad \left[\frac{kg}{s}\right]$$

For the H2: $$\dot{m}_{H2} = -\dot{m}_{H2O} \cdot \frac{mol\_mass_{H2}}{mol\_mass_{H2O}} \quad \left[\frac{kg}{s}\right]]$$

For the CO: $$\dot{m}_{CO} = -\dot{m}_{H2O} \cdot \frac{mol\_mass_{CO}}{mol\_mass_{H2O}} \quad \left[\frac{kg}{s}\right]$$

For the CO2: $$\dot{m}_{CO2} = -\dot{m}_{H2O} \cdot \frac{mol\_mass_{CO2}}{mol\_mass_{H2O}} \quad \left[\frac{kg}{s}\right]$$

For the chemical heat (endothermal):

$$\dot{q}_{chem,H2O} = \dot{n}_{H2O} \cdot \Delta H = \dot{n}_{H2O} \cdot \left(-41.2 \frac{kJ}{mol}\right) \quad [kJ]$$

Secondary heterogeneous reaction (Boudouard reaction, endothermal):

CO2 + C → 2CO, -172.5 kJ/ mol

The corresponding equation for the Boudouard reaction rate is [23]:

$$RR_C = \frac{14.5 \cdot \exp\left(-\frac{25{,}000}{T}\right) \cdot p_{CO2}}{1 + 3.4 \cdot 10^{-5} \exp\left(\frac{7{,}000}{T}\right) \cdot \sqrt{p_{CO2}}} \quad \left[\frac{mg}{cm^2 \cdot s} = \frac{10^{-2} kg}{m^2 \cdot s}\right]$$

It is questionable if this correlation holds in the higher pressure range, since it was determined for 1 bar pressure and is more relevant in the case of air ingress.

$$\dot{m}_C = -RR_{CO2} \cdot surface \quad \left[\frac{kg}{s}\right]$$

for the C: $$\dot{m}_{CO2} = \dot{m}_C \cdot \frac{mol\_mass_{CO2}}{mol\_mass_C} \quad \left[\frac{kg}{s}\right]$$

for the CO: $$\dot{m}_{CO} = 2 \cdot \dot{m}_C \cdot \frac{mol\_mass_{CO}}{mol\_mass_C} \quad \left[\frac{kg}{s}\right]$$

and the chemical heat removed from the system:

$$\dot{q}_{chem,Boudouard} = \dot{n}_C \cdot \Delta H = \dot{n}_C \cdot \left(172.5 \frac{kJ}{mol}\right) \quad [kJ]$$

It is planned to introduce the experimental results of the corrosion of graphite in steam atmosphere with the increasing burn-off, as provided in [20]. The problem here is that no dependence on the temperature or the partial pressure is provided because of the nature of the experiments. Here, the models will be improved.

5 Scenarios to be considered

For the reference plant, the scenario to be calculated is a common 2F break of a single steam generator tube. Since ATTICA3D does only simulate processes inside the reactor pressure vessel, important parameters and boundary conditions of the accident for the beginning have to be taken from other analysis in literature. Here references [13] and [24] prove to be helpful. In these publications the water ingress is also analysed and source terms for water are determined with the help of whole primary circuit (and also secondary circuit) simulations. The design basis accident will be taken as starting point. This scenario considers a double-end break of one steam generator tube that is detected and, subsequently, the steam generator will be isolated due to the two steam generator isolation valves allowing approximately 600 kg to enter the primary circuit, see [13]. Also a beyond design basis accident may be investigated, e.g. the steam generator with a total water/steam inventory of about 4000 kg between the two isolation valves (on feed water and life steam side) can enter the primary circuit.

Later in this project, the boundary conditions like mass flux of steam and inlet temperature will be taken from the analysis of a 2F break of a single steam generator tube with a two-phase system code SPECTRA. The advantage of using a two-phase system code here is the possibility of modeling the entire system (reactor vessel, steam generator, sub-systems) to calculate the transport of water and steam throughout the reactor system. This is important because using different boundary conditions might lead to completely different results (e.g. if the mass flux differs, the reactivity feedback will differ, hence the heat-up and the corrosion will also be different).

6 Annexes

Annex 1 – References

6.1 References

[1] W. Bernnat, W. Feltes, Models for reactor physics calculations for HTR pebble bed modular reactors, Nuclear Engineering and Design 222 (2003) 331–347

[2] D. Mathews, An Improved Version of the Microx-2 Code, Paul Scherer Institut, PSI Bericht Nr. 97-11, November 1997.

[3] X-5 Monte Carlo Team, MCNP – A General Monte Carlo N-Particle Transport Code, Version 5, Los Alamos National Laboratory, LA-UR-03-1987, revised 10/3/05.

[4] Rhoades, W. A., Simpson, D. B. (1991). The TORT Three dimensional Discrete Ordinates Neutron/Photon Transport Code (TORT Version 3), ORNL/TM-13221.

[5] A. Seubert, K. Velkov and S. Langenbuch, The Time-Dependent 3-D Discrete Ordinates Code TORT-TD with Thermal-Hydraulic Feedback by ATHLET Models, Physor 2008, Interlaken, Switzerland, September 14-19, 2008.

[6] Seubert, A. Sureda, J. Bader, J. Lapins, M. Buck, E. Laurien, The 3-D time-dependent transportcode TORT-TD and its coupling with the 3D thermal-hydraulic code ATTICA3D for HTGR applications, Nucl. Eng. and Design 2011, in press.

[7] The Nuclear Safety Standards Commission (Kerntechnischer Ausschuss - KTA), Reactor Core Design for High-Temperature Gas-Cooled Reactor, KTA 3102, 1983.

[8] H. Reutler and G.H. Lohnert, ADVANTAGES OF GOING MODULAR IN HTRs, Nuclear Engineering and Design 78 (1984) 129-136.

[9] Zuoyi Zhang, Zongxin Wu, Dazhong Wang, Yuanhui Xu, Yuliang Sun, Fu Li , Yujie Dong, Current status and technical description of Chinese 2×250MWth HTR-PM demonstration plant, Nuclear Engineering and Design 239 (2009) 1212–1219.

[10] H. Reutler and G.H. Lohnert, ADVANTAGES OF GOING MODULAR IN HTRs, Nuclear Engineering and Design 78 (1984) 129-136.

[11] W. A. Rhoades, R. L. Childs, The TORT Three dimensional Discrete Ordinates Neutron/Photon Transport Code, Nucl. Sci. Eng. 107, p. 397, 1991.

[12] W. A. Rhoades, D. B. Simpson, The TORT Three dimensional Discrete Ordinates Neutron/Photon Transport Code (TORT Version 3), ORNL/TM-13221, 1991.

[13] Y. Zheng, L. Shi, Y. Wang: Water-ingress analysis for the 200 MWe pebble-bed modular high temperature gas-cooled reactor, Nuclear Engineering and Design 240 (2010), pp. 3095-3107

[14] P.L. Walker Jr., F. Rusinko Jr., L.G. Austin: Gas Reactions of Carbon, Advances in Catalysis, IX, 1951, pp. 133-221

[15] K.-J. Loenißen: Untersuchungen zur Druckabhängigkeit der Graphit/Wasserdampfreaktion im Porendiffusionsbereich im Zusammenhang mit Wassereinbruchsstörfällen in Hochtemperatur-Reaktoren, Juel-2159, September 1987, ISSN 0366-0885

[16] R. C. Reid, J.M. Prausnitz, B.E. Poling; The Properties of Gases and Liquids, McGraw Hill, (1987)

[17] R. Brokaw: Approximate Formulas for the Viscosity and Thermal Conductivity of Gas Mixtures, Journal of Chemical Physics Vol. 29, No. 2, August 1958

[18] R. Moormann, K. Petersen : REACT/THERMIX – Ein Computercode zur Berechnung der störfallbedingten Graphitkorrosion in Kugelhaufenreaktoren, Juel-1782, April 1982, ISSN 0366-0885

[19] R. Nieder: Chemie des Hochtemperaturreaktors – Vorträge eines Fachseminars der KTG-Fachgruppe „Chemie und Entsorgung“ und der KFA Jülich am 5. November 1981 in Jülich, Jül-Conf-43, ISSN 0344-5798, pp. 30- 42 P. Kubaschewski, B. Heinrich: Graphitkorrosion durch Wasserdampf, Hochtemperaturreaktorbau GmbH

[20] H.-K. Hinssen, W. Katscher, K.-J. Loenißen, R. Moormann: Korrosion von graphitischen Hochtemperatur-Werkstoffen mit Wasserdampf/Helium Mischungen im Druckbereich von 3-55 bar bei Temperaturen von 900-1150°C, Juel-2747, ISSN 0366-0885

[21] W. Graven, J. Long: Kinetics and Mechanisms of the Two Opposing Reactions of the Equilibrium CO + H2O = CO2 + H2, Journal of the American Chemical Society, 76, (1954), pp. 2602-2607

[22] W. Graven, J. Long: Corrections of ‘Kinetics and Mechanisms of the Two Opposing Reactions of the Equilibrium CO + H2O = CO2 + H2’, Journal of the American Chemical Society, 76, (1954), p. 6421

[23] R. Moormann: Effects of Delays in Afterheat Removal on Consequences of Massive Air Ingress Accidents in High-Temperature Gas-Cooled Reactors

[24] D. Yujie ,Zh. Zuoyi, W. Scherer: Assessments of Water Ingress Accidents in a Modular High Temperature Gas-Cooled Reactor, Nuclear Technology 149, (2005), pp. 253-264

[25] G. H. Lohnert: The consequences of water ingress into the primary circuit of an HTR-Module – From design basis accidents to hypothetical postulates, Nuclear Engineering and Design, 134, (1992), pp. 159 - 176